The Chirality Chain in Valine: How the Configuration at the C_α Position through the $O_{cis}C'C_\alpha N$ Torsional System Leads to Distortion of the Planar Group $C_\alpha C'(O_{cis})O_{trans}$ to a Flat Tetrahedron

Henri Brunner*[a] and Takashi Tsuno*[b]

Dedicated to Prof. Dr. Manfred Scheer, the successor of Prof. Dr. Henri Brunner on the Chair of Chemistry at the University of Regensburg

Solid-state structures, based on a Cambridge Structural Database (CSD) search, show that there is a $C_\alpha N/C'O_{cis}$ attraction in the torsional system $O_{cis}C'C_\alpha N$ of valine, causing a chirality chain. The C_α configuration controls the chirality of the rotation around the $C'–C_\alpha$ bond, which in turn induces a distortion of the planar unit $C_\alpha C'(O)O$ to a flat asymmetric tetrahedron. Conformational "reactions" take place in an energy profile with respect to clockwise and counterclockwise rotation around the $C'–C_\alpha$ bond as well as stretching and flattening of the tetrahedron. The molecular property $C_\alpha N/C'O_{cis}$ attraction of valine is maintained in its di- and tripeptides.

Natural amino acids with their inherent molecular properties are the building blocks of proteins. Herein, we show that for valine, the chirality chain from the configuration at the C_α position through the torsional system $O_{cis}–C'–C_\alpha–N$, leads to the distortion of the planar group $C_\alpha C'(O_{cis})O_{trans}$ to a flat tetrahedron.

A search in the Cambridge Structural Database for $H_3N–CH(iPr)–C'(O)O$ gave 68 hits, with 28 structures containing independent molecules. Thus, 105 cases are available for analysis (these are collected in Tables S1 and S2 in the Supporting Information). As these tables comprise up to 65 entries, truncated Table 1 and Table 2 are used in this Communication.

[a] *Prof. Dr. H. Brunner*
Institut für Anorganische Chemie
Universität Regensburg
93040 Regensburg (Germany)
E-mail: henri.brunner@chemie.uni-regensburg.de

[b] *Prof. Dr. T. Tsuno*
Department of Applied Molecular Chemistry
College of Industrial Technology
Nihon University
Narashino, Chiba 275–8575 (Japan)
E-mail: tsuno.takashi@nihon-u.ac.jp

There are 40 structure determinations of valine in its zwitterionic form (see Table S1). Three representative examples of pure valine racemate and enantiomers are given at the beginning of Table 1. The valine enantiomers have two independent molecules in the unit cell, differentiated by parentheses. The second part of Table 1 contains zwitterionic valine structures in different environments, selected such that Table 1 does not exceed ten entries.

We determined the torsion angles $\psi = O_{cis}–C'–C_\alpha–N$ of the valine racemate (Table 1, entry 4) and enantiomers (entries 1 and 8). We differentiate the oxygen atoms of the carboxylic group as O_{cis} and O_{trans} according to their orientation with respect to the amino nitrogen atom (Figure 1 A). As the torsion angles ψ measure the rotation around the $C_\alpha–C'(O)O$ bond, we call them rotation angles. For L-valine in enantiomers and racemates the rotation angles ψ are negative (Figure 1 A), for D-valine they are positive. A four-atom system such as $O_{cis}–C'–C_\alpha–N$ is chiral, unless the torsion angle ψ is 0 or 180°. According to the helicity rule of the CIP system,[1] positive rotation angles result in (*P*)-conformation and negative angles in (*M*)-conformation.

The central carbon atom of the carboxylic group of valine is sp^2-hybridized. Thus, the unit $C_\alpha C'(O)O$ should be planar and achiral. However, a deviation from planarity results in a flat tetrahedron, which is chiral, due to its four different corners C′, C_α, O_{cis}, and O_{trans} (Figure 1 B). A measure of its chirality is the torsion angle $\theta = O_{trans}–C'–C_\alpha–O_{cis}$. The torsion angles θ will be called pyramidalization angles. They determine the deviation of O_{cis} from the plane $O_{trans}–C'–C_\alpha$ (Figure 1 B and 1C) due to the attraction $C_\alpha N/C'O$ (see below). The configuration of the flat tetrahedron will be specified by (*R*)/(*S*) according to the priority sequence $O_{cis} > O_{trans} > C' > C_\alpha$ of the CIP system.[1] For valine in peptides the priority sequence is $O > N > C' > C_\alpha$. The flat tetrahedron in Figure 1 B and 1C has (*S*)-configuration. Thus, the complete stereochemistry of L-valine in enantiomers and racemates is L(*M*)(*S*) and that of D-valine is D(*P*)(*R*).

In the tables, all the hits of the CSD search are included irrespective of old/new, low/high quality, because each hit is an individual structure determination. Multiple analyses help to evaluate small effects such as tetrahedral distortions. For the relatively large pyramidalization angle $\theta = 177.10°$ of AHEJEC03(2) (Table S1, entry 18), the deviation of O_{cis} from the plane $O_{trans}–C'–C_\alpha$ amounts to 0.021 Å. However, the following

Table 1. Zwitterionic valine structures.

Entry	CSD symbol[a]	Chirality chain Config. C_α	O_{cis}-C′-C_α-N rotation angle ψ [°]	O_{trans}-C′-C_α-O_{cis} pyramidal angle θ [°]	Distances [Å] O_{cis}—N	O_{cis}—C(^{i}Pr)	Attraction C_αN/C′O angles [°] *N*-C_α-C′(O)	(^{i}Pr)C-C_α-C′(O)	Comments
1	LVALIN01(1)	L	−17.48	−177.78	2.66	3.39	109.26	112.72	enantiomer(1)
4	VALIDL03	L	−23.31	−179.09	2.67	3.33	110.02	112.47	racemate[b]
8	LVALIN01(2)	L	−42.81	−177.66	2.76	3.10	109.33	110.48	enantiomer(2)
12	AHEJEC(1)[c]	D	17.95	177.75	2.66	3.38	109.31	112.98	enantiomer(1)
18	AHEJEC03(2)[c]	D	43.99	177.82	2.75	3.09	109.23	110.74	enantiomer(2)
20	OPEFUL[1]	L	−5.53	−181.00	2.60	3.51	107.19	116.10	+ L-valine·HCl adduct
25	GUQJUZ[1](2)	L	−20.39	−177.28	2.64	3.30	107.90	112.64	+ valine·naphthalene-1,5-$(SO_3H)_2$ adduct
30	GOLVUY	L	−35.59	−177.34	2.69	3.17	108.04	110.44	+ D-n-BuAA[d]
40	SONCED[c]	D	25.84	179.48	2.68	3.31	109.52	112.63	+ L-phenylalanine
	average		−27.74	−178.32	2.69	3.28	108.86	111.95	

[a] Parenthesis () indicate independent molecules in the unit cell, whereas brackets [] differentiate between $^+NH_3CH(^iPr)COO^-$ and $^+NH_3CH(^iPr)COOH$. [b] Racemates given as L-compounds. [c] For average calculation rotation angle and distortion angle are inverted. [d] AA = amino acid.

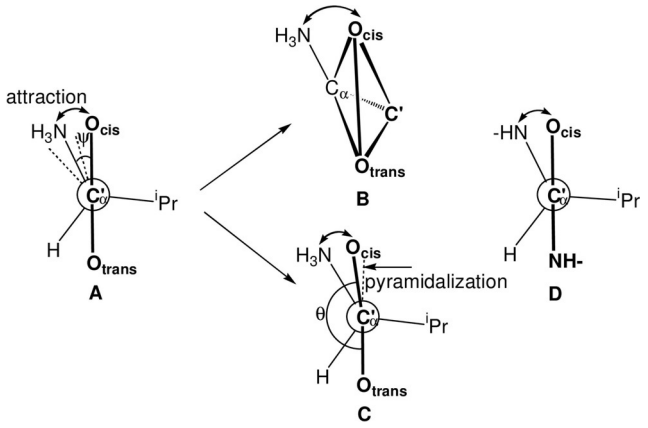

Figure 1. A) Rotation angles $\psi = O_{cis}$–C′–C_α–N in the zwitterionic racemate and enantiomers (dashed) of L-valine (Table 1, entries 1, 4, 8), looking down the C′–C_α bond (symbol C′$_\alpha$). B) Distortion of the planar system C_αC′(O)O to a chiral flat tetrahedron (exaggerated). C) Attraction C_αN/C′O: bending of C′–O_{cis} towards C_α–NH_3. D) Conformation of valine in di- and tripeptides.

analysis will show that both the induction from the given chirality at C_α to the torsional system O_{cis}C′C_αN and from the torsional system to the pyramidalization of the planar group C_αC′(O)O occurs with high diastereoselectivity.

The second part of Table 1 shows structures in which the valine zwitterion crystallizes together with L-valine molecules protonated by strong acids or co-crystallizes with natural and unnatural amino acids. In all cases the induction chain L→(−)→(−) is perfect. In the 40 cases of Table S1, there is one example in which the rotation angle ψ adopts a small positive value, inducing (*P*)-configuration in the flat tetrahedron. Concerning the induction from the torsional system to the flat tetrahedron there are four exceptions ($\theta > -180°$).

In entries 1–40 of Tables 1 and S1 the valine zwitterion is in completely different environments. Irrespective of the changing packing and hydrogen-bond networks, a unique structural motif is common to all structures, the chiral induction chain. The given L/D-chirality at the C_α position controls the arrangement of the torsional system O_{cis}C′C_αN in the narrow range from 3.49° to −53.26° of rotation angles ψ. The other 303° of the full circle are not occupied by sample points. The torsional system O_{cis}C′C_αN in turn induces the preferred (*S*)-configuration in the flat tetrahedron with high selectivity.

Strong acids protonate valine at the carboxylic group to give salt-like structures with the cation H_3N-CH(*i*Pr)-C′(O)OH^+. In all the structures of Tables 2 and S2 (54 cases), protonation occurs on the O_{trans} atom except for HOSMEA (entry 54). In three cases, the O_{trans} centre is alkylated to give the methyl and benzyl esters (entries 39, 40, and 46). Protonation and alkylation differentiate O_{cis} and O_{trans} with respect to the lengths of the C′–O bonds. The C′–O bonds are much longer in the COH/R system compared to the C=O group.

The range of rotation angles ψ in Tables 2 and S2 from 1.77° to −43.91° is even a little narrower than in Tables 1 and S1. According to the chirality chain, the two slightly positive rotation angles in entries 1 and 2 induce positive pyramidal angles. The 49 negative rotation angles from entry 3 to entry 52 in the L-valine series result in negative pyramidal angles (9 exceptions; $\theta > -180°$). Thus, the results in Tables 2 and S2 corroborate the high selectivities in protonation as well as rotation and pyramidalization angles.

At the end of Table S2 (see the Supporting Information) eleven structures are listed in which valine zwitterions coordinate as ligands in metal complexes. The induction from the C_α position to the torsional system O_{cis}C′C_αN is perfect; from the torsional system to the flat tetrahedron there are two exception ($\theta > -180°$).

In Table S1 (see the Supporting Information) there is one L-Val with a positive rotation angle and Table S2 contains two L-Val entries with slightly positive rotation angles. They are the positive parts of the range from −53.26° to 3.49°, which is well in agreement with the fact that the C_α configuration confers induction onto the torsional system O_{cis}C′C_αN. However, the chirality of the torsional system O_{cis}C′C_αN changes from (*M*) for −53.26–0° to (*P*) for 0–3.49°.

In the torsional system O_{cis}C′C_αN of the valine zwitterions, the C_α–NH_3 bond is close to eclipsing the C′–O_{cis} bond, indicating an attraction C_α–NH_3/C′–O_{cis}. This is evident in the small

Table 2. Valine zwitterions protonated at the carboxylic group by strong acids.

Entry	CSD symbol[a]	Chirality chain Config. C_α	O_{cis}-C′-C_α-N rotation angle ψ [°]	O_{trans}-C′-C_α-O_{cis} pyramidal angle θ [°]	Distances [Å] O_{cis}—N	O_{cis}—C(^{i}Pr)	Attraction C_αN/C′O angles [°] *N*-C_α-C′(O)	(^{i}Pr)C-C_α-C′(O)	Comments
1	WIHQUA(1)	L	1.77	−182.10	2.66	2.66	107.24	111.77	H_2NbOF_5
8	VALHCL10	L	−3.72	−182.11	2.68	2.68	108.41	109.80	HCl, H_2O
16	TUZJIJ	L	−11.44	−177.98	2.65	2.65	107.86	110.89	TsOH, H_2O
24	WIHQUA(2)[b]	L	−15.68	−178.90	2.68	2.68	107.69	113.46	H_2NbOF_5
32	BANPOW(4)	L	−20.98	−177.94	2.69	2.69	107.69	110.13	$HClO_4$
40	DUMZOB	L	−25.00	−179.10	2.71	2.71	107.07	113.47	HCl, Bn ester
48	ROKBOI(2)	L	−32.49	−179.22	2.76	2.76	108.63	109.72	HNO_3
56	ESAPET01(1)	L	−14.91	−179.54	2.65	2.65	110.26	112.59	H_2PbO_3, $2HNO_3$, H_2O
65	VALCAC	L	−35.46	−179.94	2.67	2.67	105.99	110.48	$CaCl_2(H_2O)$
	average		−18.69	−179.06	2.67	3.36	107.69	112.38	

[a] Parenthesis () indicate independent molecules in the unit cell. [b] Racemates given as L-compounds.

negative rotation angles ψ (average $\psi = -27.74^\circ$ in Table S1, $\psi = -18.69^\circ$ in Table S2, and average $\psi = -22.13^\circ$ in Tables S1 and S2, see the Supporting Information). We think the attraction is due to NH…O_{cis} hydrogen bonding.

The attraction C_α—NH_3/C′—O_{cis} should manifest itself also in structural parameters like distances and bond angles. In the torsional system O_{cis}C′C_αN, proof for an attraction comes from the distances O_{cis}—N and O_{cis}—C(*i*Pr) in Tables 1 and S1 and Tables 2 and S2 (columns 6 and 7; see the Supporting Information). Increasing the rotation angle ψ from 0 to −53° should increase the distances O_{cis}—N and decrease the distances O_{cis}—C(*i*Pr) in the same way. However, excluding the outlier 2.48 Å (see Table S2, entry 13 in the Supporting Information), the interval of the distances O_{cis}—N spans only 0.2 Å from 2.60–2.82 Å, whereas the interval of the distances O_{cis}—C(*i*Pr) overstretches 0.6 Å from 3.00–3.60 Å. This shows that the torsional system O_{cis}C′C_αN resists elongation of the distance O_{cis}—N by adjusting bond lengths and angles such as to keep the distance O_{cis}—N as constant as possible. As the van der Waals radii of O and N are 1.55 and 1.60 Å,[2] the O_{cis}—N distances are far below the sum of the van der Waals radii, indicating an attractive interaction in the torsional system O_{cis}C′C_αN.

In columns 8 and 9 of Tables 1 and S1, the bond angles *N*-C_α-C′(O) and (*i*Pr)C-C_α-C′(O) are compared. The *N*-C_α-C′(O) angles are generally below the tetrahedral angle (average 108.86°; see Table S1) and smaller than the (*i*Pr)C-C_α-C′(O) angles, which are above the tetrahedral angle (average 111.95°). Tables 2, 3 and Tables S2 and S3 show the same trends. As the size of the isopropyl substituent could be a reason for the large angles (*i*Pr)C-C_α-C′(O), we checked the 78 zwitterionic structures of alanine in the CSD. In alanine, C_α—NH_3 and C_α—CH_3 have similar sizes. The averages of the angles H_3N-C_α-C′(O) and H_3C-C_α-C′(O) in alanine are 109.70° and 111.44°,[3] confirming the attraction C_α—NH_3/C′—O_{cis}, which in turn is the reason for the chirality transfer from the C_α configuration to the torsional system O_{cis}C′C_αN.

Thus, distances and torsion as well as bond angles prove the attraction C_α—NH_3/C′—O_{cis}, in which C′—O_{cis} and C_α—NH_3 bend towards each other (Figure 1C) in valine and also in alanine.

The 105 sample points of Tables S1 and S2 are shown in the histogram of Figure 2. L-compounds crowd in the lower right quadrant. In Figure 2 the D-compounds are inverted to L-compounds. Exceptions appear in the lower left quadrant. The best-fit line of the 102 compounds with negative rotation angles indicates a good correlation of rotation and pyramidalization angles (step 2 of the chirality chain). The best-fit line is additional proof for the attraction C_α—NH_3/C′—O_{cis}. It shows that the more the O_{cis} centre is removed from the perpendicular plane O_{trans}C′C_α in Figure 1C, the larger the torsion angle ψ.

Movement along the best-fit line in Figure 2 describes readily occurring conformational changes as exemplified for the "reaction" HURXEX(1) → ROKBOI02(4). The descent from HURXEX(1) to ROKBOI02(4) along the best-fit line implies a ro-

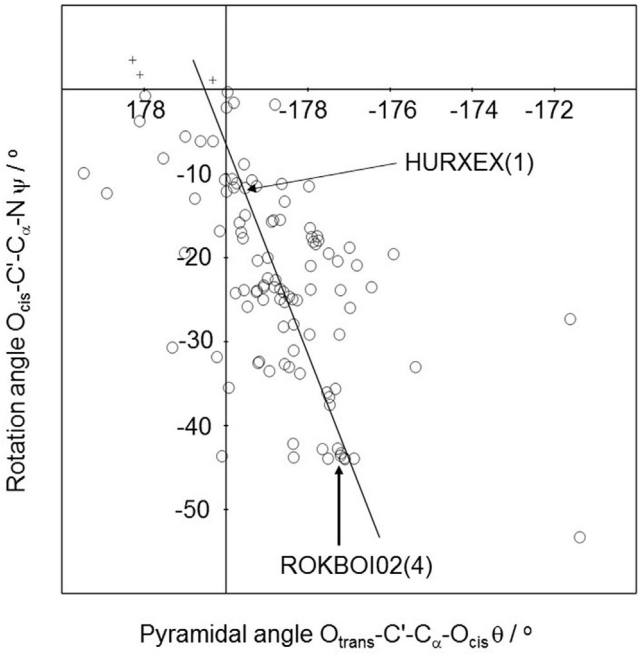

Figure 2. Histogram of the correlation of rotation angles (ordinate) and pyramidalization angles (abscissa) of the 105 sample points of Tables S1 and S2. D-compounds inverted to L-compounds ($R^2 = 0.2944$, $\rho < 3.85 \times 10^{-9}$;102 compounds with negative rotation angles).

tation around the C′–C_α axis in a specific direction and an increasing distortion of the flat tetrahedron. Rotation around the C′–C_α axis of HURXEX(1) from −11.68° to −43.91° of ROKBOI02(4) is a counter-clockwise (c-clw) movement of 32.23°. It is associated with a stretching of the flat tetrahedron, indicated by an increase of the pyramidalization angle from 179.51° to 176.71° (Figure 3). The other way round, the ascent from HURXEX(1) to ROKBOI02(4) is a clockwise rotation around C′–C_α combined with a compression of the flat tetrahedron.

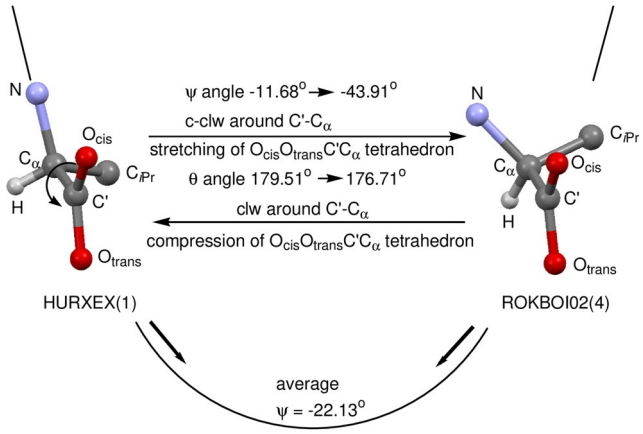

Figure 3. Conformational "reactions" HURXEX(1)→ROKBOI02(4) and ROKBOI02(4)→HURXEX(1).

In Figure 3 the reaction HURXEX(1) → ROKBOI02(4) is embedded in an energy profile with respect to rotation around the C′–C_α bond in valine. The accumulation of sample points is interpreted as the energy minimum.[4,5] Following the arrows towards the energy minimum, conformations of type HURXEX(1) rotate preferentially counter-clockwise stretching the flat tetrahedron, whereas those of type ROKBOI02(4) rotate clockwise flattening the tetrahedron.

Table 3 summarizes rotation and pyramidalization angles as well as distances and bond angles of valine-containing tripeptides (Figure 1 D). There is not much difference between valine at the amino end, in the middle or at the carboxy end and the results are well in line with the valine structures in Tables S1 and S2.

All the rotation angles of valine in the tripeptides are negative except for entry 1 (Table 3), which contains D-valine at the amino end. They span the typical range from −0.79° to −58.51°. The (*M*)-torsional system induces (*S*)-chirality in the flat tetrahedron with one exception, the value −179.8° of which is close to −180°. The distances O_{cis}–N are short and the bond angles *N*-C′-C_α are far below the tetrahedral angle due to the attraction C_αN/C′O_{cis}.

As the analysis of valine-containing dipeptides comprises 78 examples, Table S3 is given in the Supporting Information. The results correspond to those obtained up to now. The range of rotation angles is from 6.45° to −71.60° except for MOBYEH, which contains 8 independent molecules, four of which have the expected small negative rotation angles. However, four MOBYEH molecules have the unfavorable *syn*-conformation with respect to the C′–C_α bond, which entails large rotation angles. The selectivity of distortion of the flat tetrahedron is better than 80%. The distances O_{cis}–N and O_{cis}–C(*i*Pr) as well as the angles *N*–C′–C_α and (*i*Pr)C–C_α–C′(O), confirming the attraction C_αN/C′O_{cis}, are comparable to Tables S1 and S2.

Pyramidalization of the unit C_αC′(O)O in Val is caused by the C_α–N/C′–O_{near} attraction. There are other weak interactions, resulting in pyramidalizations, for example, n→π* interactions. In proteins, the approach of an adjacent C=O group to the C′ po-

Table 3. Valine in tripeptides.

Entry	CSD symbol[a]	Tripeptide	Chirality chain Config. C_α	O_{cis}-C′-C_α-N ψ [°]	$O_{trans}(N_{amide})$-C′$_\alpha$-O_{cis} θ [°]	Distances [Å] O_{cis}–N	O_{cis}–C(^{i}Pr)	Attraction C_αN/C′O angles [°] *N*-C_α-C′(O)	(^{i}Pr)C-C_α-C′(O)	Comments
1	DVLTLV10[b]	Val-Trp-Val	DLL	15.58	177.88	2.87	3.07	107.25	110.44	amino end (D)
2	AQOWAE	Val-Gly-Gly	L	−0.79	−179.35	2.70	3.52	109.44	111.35	carboxy end, HCl
3	BEVYIL	Val-Val-Val	LLL	−31.74	−176.74	2.75	3.26	109.74	109.47	carboxy end, CF_3COOH
4	XEPZAU(1)	Val-Ile-Ala	LLL	−42.92	−177.06	2.74	3.15	107.71	112.67	
5	BEVYIL	Val-Val-Val	LLL	−43.80	−176.67	2.76	3.06	107.23	108.82	amino end, CF_3COOH
6	XEPZAU(2)	Val-Ile-Ala	LLL	−44.68	−174.99	2.74	3.08	107.34	110.63	
7	XEPZAU(3)	Val-Ile-Ala	LLL	−46.51	−178.50	2.74	3.05	105.97	110.19	
8	XEPZAU(4)	Val-Ile-Ala	LLL	−47.69	−177.44	2.76	3.05	106.91	110.16	
9	BEVYIL	Val-Val-Val	LLL	−50.01	−177.49	2.81	3.06	108.95	110.31	carboxy end
10	CUWRUH	Gly-Gly-Val	L	−50.71	−180.21	2.86	3.11	110.28	111.96	
11	DVLTLV10	Val-Trp-Val	DLL	−52.20	−178.29	2.62	3.35	110.03	111.68	carboxy end (L)
12	BEVYIL	Val-Val-Val	LLL	−54.03	−178.68	2.82	3.03	106.78	109.25	middle CF_3COOH
13	BEVYIL	Val-Val-Val	LLL	−54.47	−176.94	2.89	2.96	106.41	108.78	amino end
14	COPBIS10	Val-Gly-Gly	L	−58.32	−178.58	2.86	3.00	107.05	110.78	amino end
15	BEVYIL	Val-Val-Val	LLL	−58.51	−179.75	2.84	3.01	106.02	110.55	middle
	Average			−43.46	−177.91	2.78	3.12	107.81	110.47	

[a] Parenthesis ( ) indicate independent molecules in the unit cell. [b] For average calculation rotation angle and pyramidalization angle inverted.

sition of a carboxamide below 3.22 Å is considered a weak non-covalent n→π* attraction.[6] In the dipeptides of Table S3, three such pyramidalizations by n→π* interactions are present (entries 5, 10, 28).

The small negative ψ angle and the induced (*S*)-pyramidalization, controlled by the configuration at the C_α position and the attraction C_α–N/C′–O_{cis}, are inherent properties of the L-Val molecule, which may be overruled in proteins by other effects. Thus, valine enters into α-helix domains with small negative ψ angles and (*S*)-pyramidalization. However, when valine is used as a building block in β-sheet domains, dramatic changes in the ψ angles and a chirality change of the pyramidalization takes place.[7,8]

As other amino acids show similar effects as valine, further studies are in progress.

Experimental Section

The Cambridge Structural Database ver. 5.39[9] (update May 2018) was used for a search of the compounds in Tables 1–3 and Tables S1–S3. The programs *OLEX*^{2},[10] Mercury CSD ver. 3.10.2,[11] and ConQuest ver. 1.22[12] were used for the structure analyses.

Conflict of Interest

The authors declare no conflict of interest.

Keywords: amino acids · chirality · conformation · peptides · valine

[1] R. S. Cahn, C. Ingold, V. Prelog, *Angew. Chem. Int. Ed. Engl.* **1966**, *5*, 385–415; *Angew. Chem.* **1966**, *78*, 413–447.
[2] S. Alvarez, *Dalton Trans.* **2013**, *42*, 8617–8636.
[3] Publication in preparation.
[4] E. Bye, B. Scheizer, J. D. Dunitz, *J. Am. Chem. Soc.* **1982**, *104*, 5893–5898.
[5] H. Brunner, G. Balázs, T. Tsuno, H. Iwabe, *ACS Omega* **2018**, *3*, 982–990.
[6] R. W. Newberry, R. T. Raines, *Acc. Chem. Res.* **2017**, *50*, 1838–1846.
[7] L. Esposito, L. Vitagliano, A. Zagari, L. Mazzarella, *Protein Sci.* **2000**, *9*, 2038–2042.
[8] S. A. Hollingsworth, P. A. Karplus, *Biomol. Concepts* **2010**, *1*, 271–283.
[9] C. R. Groom, I. J. Bruno, M. P. Lightfoot, S. C. Ward, *Acta Crystallogr. Sect. B* **2016**, *B72*, 171–179.
[10] O. V. Dolomanov, L. J. Bourhis, R. J. Gildea, J. A. K. Howard, H. J. Puschmann, *Appl. Crystallogr.* **2009**, *42*, 339–341.
[11] C. F. Macrae, I. J. Bruno, J. A. Chisholm, P. R. Edgington, P. McCabe, E. Pidcock, L. Rodriguez Monge, R. Taylor, J. van de Streek, P. A. Wood, *J. Appl. Crystallogr.* **2008**, *41*, 466–470.
[12] I. J. Bruno, J. C. Cole, P. R. Edgington, M. Kessler, C. F. Marcrae, P. McCabe, J. Pearson, R. Taylor, *Acta Crystallogr. Sect. B* **2002**, *B58*, 389–397.